

UC Berkeley

UC Berkeley Previously Published Works

Title

Status of the MAJORANA DEMONSTRATOR

Permalink

<https://escholarship.org/uc/item/2sq7g3x8>

Journal

Physics of Particles and Nuclei, 48(1)

ISSN

1063-7796

Authors

Vasilyev, S
Abgrall, N
Arnquist, IJ
[et al.](#)

Publication Date

2017

DOI

10.1134/s1063779616060253

Peer reviewed

Status of the MAJORANA DEMONSTRATOR (MJD)

S. Vasilyev¹, N. Abgrall², I.J. Arnquist³, F.T. Avignone III^{4,5},
C.X. Balderrot-Barrera⁵, A.S. Barabash⁶, F.E. Bertrand⁵, A.W. Bradley²,
V. Brudanin¹, M. Busch^{8,9}, M. Buuck¹⁰, D. Byram¹¹, A.S. Caldwell¹²,
Y-D. Chan², C.D. Christofferson¹², C. Cuesta¹⁰, J.A. Detwiler¹⁰,
Yu. Efremenko⁷, H. Ejiri¹³, S.R. Elliott¹⁴, A. Galindo-Uribarri⁵, T. Gilliss^{9,15},
G.K. Giovanetti^{9,15}, J. Goett¹⁴, M.P. Green⁵, J. Gruszko¹⁰, I. Guinn¹⁰,
V.E. Guiseppe⁴, R. Henning^{9,15}, E.W. Hoppe³, S. Howard¹², M.A. Howe^{9,15},
B.R. Jasinski¹¹, K.E. Keeter¹⁶, M.F. Kidd¹⁷, S.I. Kononov⁶, R.T. Kouzes³,
B.D. LaFerriere³, J. Leon¹⁰, J. MacMullin^{9,15}, R.D. Martin¹¹, S.J. Meijer^{9,15},
S. Mertens², J.L. Orrell³, C. O'Shaughnessy^{9,15}, A.W.P. Poon², D.C. Radford⁵,
J. Rager^{9,15}, K. Rielage¹⁴, R.G.H. Robertson¹⁰, E. Romero-Romero^{7,5},
B. Shanks^{9,15}, M. Shirchenko¹, N. Snyder¹¹, A.M. Suriano¹², D. Tedeschi⁴,
J.E. Trimble^{9,15}, R.L. Varner⁵, K. Vetter², K. Vorren^{9,15}, B.R. White⁵,
J.F. Wilkerson^{5,9,15}, C. Wiseman⁴, W. Xu¹⁴, E. Yakushev¹, C-H. Yu⁵,
V. Yumatov⁶, and I. Zhitnikov¹

The MAJORANA Collaboration

¹*Joint Institute for Nuclear Research, Dubna, Russia*

²*Nuclear Science Division, Lawrence Berkeley National Laboratory, Berkeley, CA, USA*

³*Pacific Northwest National Laboratory, Richland, WA, USA*

⁴*Department of Physics and Astronomy, University of South Carolina, Columbia, SC, USA*

⁵*Oak Ridge National Laboratory, Oak Ridge, TN, USA*

⁶*Institute for Theoretical and Experimental Physics, Moscow, Russia*

⁷*Department of Physics and Astronomy, University of Tennessee, Knoxville, TN, USA*

⁸*Department of Physics, Duke University, Durham, NC, USA*

⁹*Triangle Universities Nuclear Laboratory, Durham, NC, USA*

¹⁰*Center for Experimental Nuclear Physics and Astrophysics and Department of Physics, University of Washington, Seattle, WA, USA*

¹¹*Department of Physics, University of South Dakota, Vermillion, SD, USA*

¹²*South Dakota School of Mines and Technology, Rapid City, SD, USA*

¹³*Research Center for Nuclear Physics and Department of Physics, Osaka University, Ibaraki, Osaka, Japan*

¹⁴*Los Alamos National Laboratory, Los Alamos, NM, USA*

¹⁵*Department of Physics and Astronomy, University of North Carolina, Chapel Hill, NC, USA*

¹⁶*Department of Physics, Black Hills State University, Spearfish, SD, USA*

¹⁷*Tennessee Tech University, Cookeville, TN, USA*

The MAJORANA Collaboration is constructing the MAJORANA DEMONSTRATOR, an ultra-low background, 40-kg modular high purity Ge (HPGe) detector array to search for neutrinoless double-beta decay ($0\nu\beta\beta$ -decay) in ^{76}Ge and to demonstrate a background rate at or below 3 counts/(ROI-t-y) in the 4 keV region of interest (ROI) around the 2039 keV Q-value for ^{76}Ge $0\nu\beta\beta$ -decay. In this paper, the status of the MJD, including its design and measurements of properties of the HPGe crystals is presented.

1 Introduction

Neutrinoless double-beta decay is the most general, model independent method to search for lepton number violation and correspondingly to determine the Dirac-Majorana nature of the neutrino [1, 2]. Furthermore, the Majorana nature of the neutrino would allow for the see-saw mechanism [3, 4] to explain the, seemingly finely-tuned, small neutrino masses. Finally, the rate of $0\nu\beta\beta$ -decay could be used to determine the neutrino mass scale [5]. The $0\nu\beta\beta$ -decay rate may be written as:

$$(T_{1/2}^{0\nu})^{-1} = G^{0\nu} |M_{0\nu}|^2 \left(\frac{\langle m_{\beta\beta} \rangle}{m_e} \right)^2 \quad (1)$$

where $G^{0\nu}$ is a phase space factor including the couplings, $M_{0\nu}$ is a nuclear matrix element, m_e is the electron mass, and $m_{\beta\beta}$ is the effective Majorana neutrino mass. The latter is given by

$$\langle m_{\beta\beta} \rangle = \left| \sum_{i=0}^3 U_{ei}^2 m_i \right| \quad (2)$$

where U_{ei}^2 specifies the admixture of neutrino mass eigenstate i in the electron neutrino. Then, assuming that $0\nu\beta\beta$ -decay is mainly driven by the exchange of light Majorana neutrinos, it is possible to establish an absolute scale for the neutrino mass, provided that nuclear matrix elements are known.

Experimentally, $0\nu\beta\beta$ -decay can be detected by searching the spectrum of the summed energy of the emitted electrons for a monoenergetic line at the Q-value of the decay ($Q_{\beta\beta}$). In previous-generation searches, the most sensitive limits on $0\nu\beta\beta$ -decay came from the Heidelberg-Moscow experiment [6], and the IGEX experiment [7], both using ^{76}Ge . A direct observation of $0\nu\beta\beta$ -decay was claimed by subgroup of the Heidelberg-Moscow collaboration [8]. Recent sensitive searches for $0\nu\beta\beta$ have been carried out in ^{76}Ge (GERDA

23 [9]) and ^{136}Xe (KamLAND-Zen [10] and EXO-200 [11]), setting sensitive
 24 limits that do not support such a claim.

25 The sensitivity of a $0\nu\beta\beta$ search increases with the exposure of the ex-
 26 periment, but ultimately depends on the achieved background level. This
 27 relationship is illustrated in Fig. 1, where the Feldman-Cousins [12] defi-
 28 nition of sensitivity was used in order to transition smoothly between the
 29 background-free and background-dominated scenarios.

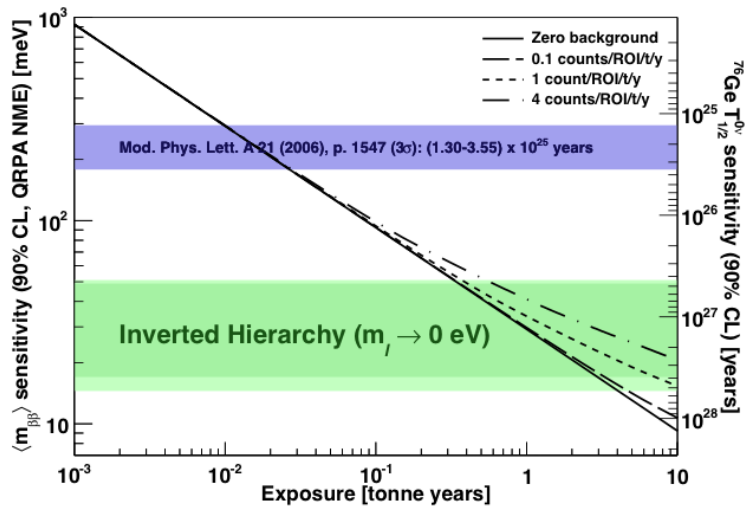


Figure 1: 90% C.L. sensitivity as a function of exposure for $0\nu\beta\beta$ -decay searches in ^{76}Ge under different background scenarios. The matrix element from Ref. [13] was used to convert half-life to neutrino mass. The upper shaded band shows the region where a signal would be detected should Klapdor-Kleingrothaus claim [8] be correct. m_l in the lower shaded band refers to the lightest neutrino mass.

30 In order to reach the neutrino mass scale associated with the inverted
 31 mass hierarchy, 15-50 meV, a half-life sensitivity greater than 10^{27}y is re-
 32 quired. This corresponds to a signal of a few counts or less per tonne-
 33 year in the $0\nu\beta\beta$ peak. Observation of such a small signal will require
 34 tonne-scale detectors with background contributions at or below a rate of
 35 1 count/(ROI-t-y).

36 2 The MAJORANA DEMONSTRATOR

37 2.1 Overview

38 The MAJORANA DEMONSTRATOR [14] is an array of enriched and natural ger-
39 manium detectors that will search for the $0\nu\beta\beta$ -decay of ^{76}Ge . The specific
40 goals of the MJD are:

- 41 • Demonstrate a path forward to achieving a background rate at or below
42 1 count/(ROI-t-y) in the 4 keV region of interest around the 2039 keV
43 $Q_{\beta\beta}$ of the ^{76}Ge $0\nu\beta\beta$ -decay.
- 44 • Show technical and engineering scalability toward a tonne-scale instru-
45 ment.
- 46 • Field an array that provides sufficient to test the Klapdor-Kleingrothaus
47 claim to be comparable with alternate approaches.
- 48 • Perform searches for other physics beyond the standard model, such as
49 dark matter and axions.

50 To this end, the collaboration is building the DEMONSTRATOR, a modular
51 instrument composed of two cryostats built from ultra-pure electroformed
52 copper, each of which can house over 20 kg of HPGe detectors contained
53 in an ultra-low background structure that maximizes the concentration of
54 crystals while minimizing the amounts of structural materials. Cryostats
55 are mounted on moveable transporters allowing independent assembly and
56 testing before installation into the shield. The array will contain about 30 kg
57 of detectors fabricated from 87% enriched ^{76}Ge and 10 kg of detectors from
58 natural Ge (7.8% ^{76}Ge).

59 Starting from the innermost cavity, the cryostats will be surrounded by
60 an inner layer of electroformed copper (5 cm), an outer layer of Oxygen-Free
61 High thermal Conductivity (OFHC) copper (5 cm), high-purity lead (45 cm),
62 an active muon veto (nearly 4π), borated polyethylene (5 cm), polyethylene
63 (25 cm) (see Fig. 2). The cryostats, copper, and lead shielding will all be
64 enclosed in a radon exclusion box. The Rn enclosure is a gas barrier whose
65 internal volume will be continuously purged with liquid nitrogen boil-off gas
66 to reduce Rn levels near the cryostats. The entire experiment will be located
67 in a clean room at the 1478 m level of the Sanford Underground Research
68 Facility (SURF) in Lead, South Dakota, USA.

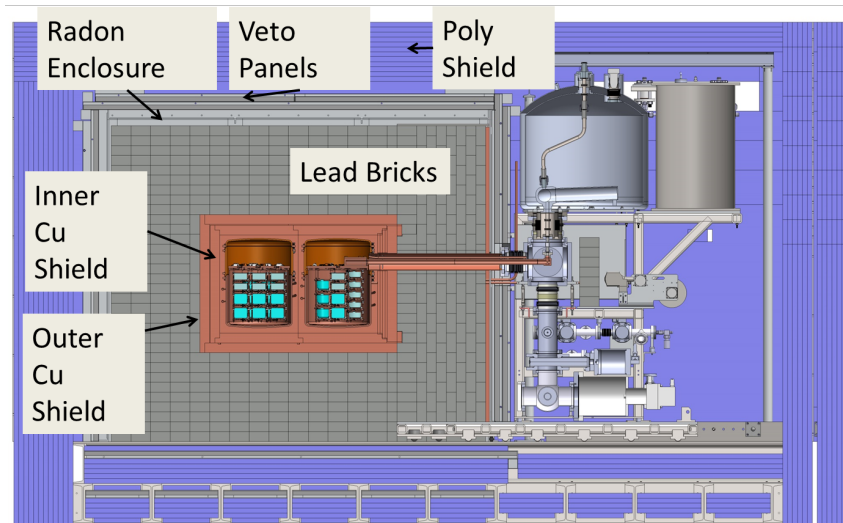


Figure 2: Cross-sectional view of the MAJORANA DEMONSTRATOR.

69 An essential aspect of the DEMONSTRATOR is the production and use of
 70 ultra-clean Cu. In typical materials uranium (U) and thorium (Th) decay-
 71 chain contaminants are found at levels of $\mu\text{g/g}$ to ng/g , which will produce
 72 unacceptable background in the DEMONSTRATOR. Electroforming copper in a
 73 carefully-controlled and clean environment allows one to produce copper with
 74 U and Th below the level of 10^{-12} g/g [15]. The copper being produced by
 75 MAJORANA has about ten times lower U and Th impurities than commercial
 76 electroformed copper, with a projected activity of $0.3 \mu\text{Bq/kg}$ for Th or lower.
 77 To avoid cosmogenic activation of the most sensitive parts, the copper is
 78 being produced at an underground (UG) production facility at SURF and
 79 at a shallow facility at Pacific Northwest National Laboratory, and is being
 80 machined UG in an ultra-clean machine shop installed and operated by the
 81 collaboration. Copper has mechanical, thermal, and electrical properties that
 82 are suitable for the DEMONSTRATOR's cryostats, detector mounts, and inner
 83 shield.

84 2.2 P-type Point-contact HPGe detectors

85 The DEMONSTRATOR uses p-type point-contact (PPC) HPGe detectors [16,
 86 17] that have masses in the range of 0.6-1.1 kg. PPC style detectors were
 87 chosen after extensive R&D by the collaboration for their advantages: simple
 88 fabrication, excellent pulse shape discrimination between $0\nu\beta\beta$ events and
 89 backgrounds, and very low capacitance, providing a low-energy threshold
 90 that allows the reduction of background from cosmogenic ^{68}Ge .

91 These detectors have all the benefits of coaxial HPGe detectors tradi-
 92 tionally used for $\beta\beta(0\nu)$, but also possess superb pulse shape analysis (PSA)
 93 discrimination between single-site interactions (such as $\beta\beta(0\nu)$ -decay events)
 94 and multi-site interaction events (such as Compton scattering of γ -ray back-
 95 grounds), making them highly suitable for $\beta\beta(0\nu)$ searches. Measured signals
 96 from a PPC detector are shown in Fig. 3.

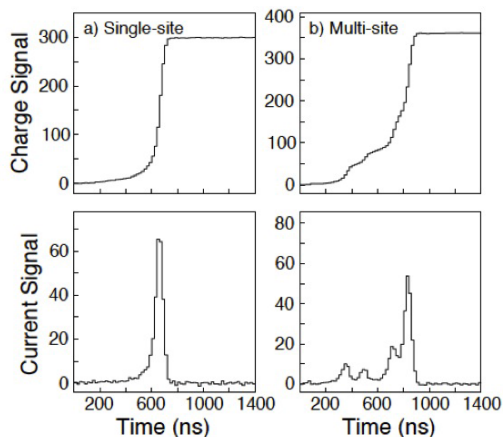


Figure 3: Charge and current pulse response of a PPC detector to single- and multi-site γ -ray events.

97 Both charge and current pulses are shown, for both a single-site (a) and a
 98 multi-site (b) γ -ray events. The difference in signal shape is readily apparent,
 99 with four distinct interactions evident in (b). The MAJORANA Collaboration
 100 uses two different types of PSA algorithm to discriminate between these two
 101 classes of events. The first of these, developed by the GERDA collaboration
 102 [18], compares the maximum height of the current pulse (A) to the total
 103 energy of the event (E) as determined from the height of the charge pulse.

104 Multiple interactions result in multiple charge pulses separated in time, and
105 therefore in a reduced value of A/E.

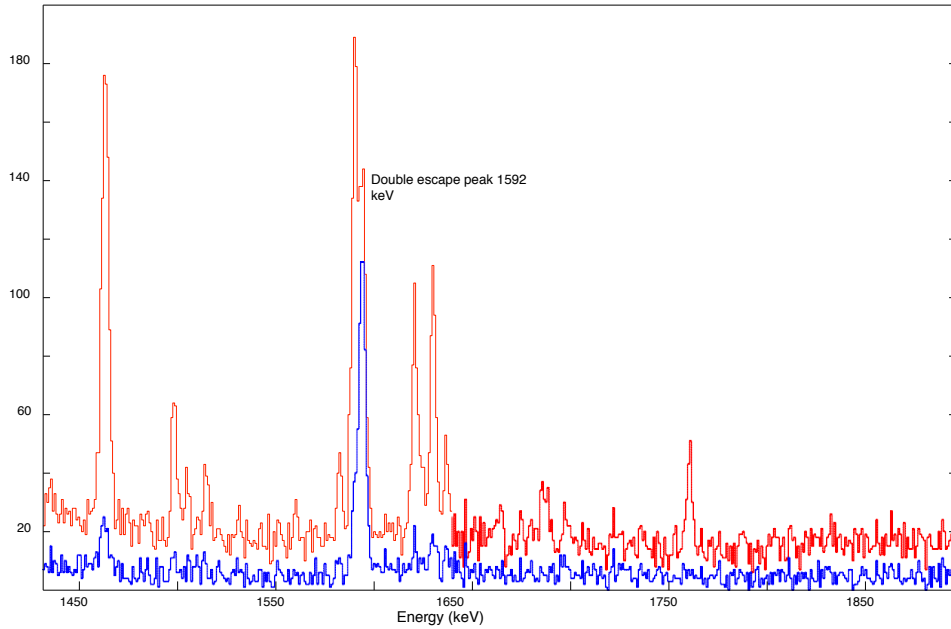


Figure 4: Pulse-shape analysis results for PPC data. The high spectrum is for all events within the energy range, while the low spectrum is for events that pass the PSA cut.

106 An alternative approach [19] uses a library of unique, measured single-site
107 signals to perform event-by-event χ^2 fitting of experimental pulse shapes. A
108 method for building this library from a large number of measured signals has
109 been developed and tested with simulation and experimental studies. Results
110 of this optimized PSA algorithms on PPC data are shown in Fig. 4, where
111 the high spectrum is all events from a ^{232}Th source, and the low spectrum is
112 for events that pass the PSA cut. The peak at 1592 keV is the double-escape
113 peak from the pair production interaction of the 2615 keV gamma-ray in

114 ^{208}Tl , the final daughter in the chain. The double-escape peak has a similar
 115 two- β event topology and serves as a proxy for the $0\nu\beta\beta$ -decay signal. The
 116 algorithm retains at least 95% of these events, while rejecting up to 99% of
 117 the single-escape, multi-site events. One should compare this to the A/E
 118 results of Ref. [18] where the double-escape peak events are accepted at 89%
 119 and the single-escape peaks are rejected at 93%. The conclusion from these
 120 measurements is that pulse shape analysis is a very effective background
 121 reduction technique with point-contact Ge detectors.

122 3 Status of the MAJORANA DEMONSTRATOR

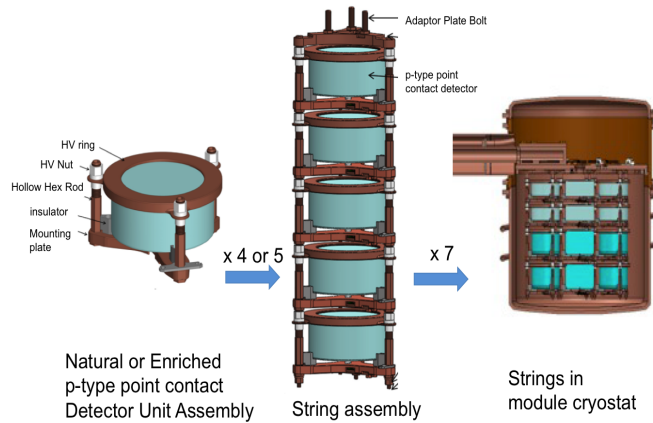


Figure 5: The modular approach of MAJORANA DEMONSTRATOR.

123 The MAJORANA Collaboration choose to use a modular approach to con-
 124 struct the experimental apparatus. Four or five individual HPGe detectors
 125 and their associated low-mass low-radioactivity mounting structures and elec-
 126 tronics are stacked together into one string assembly, and seven string assem-
 127 blies are installed into one cryostat, as shown in Fig. 5.

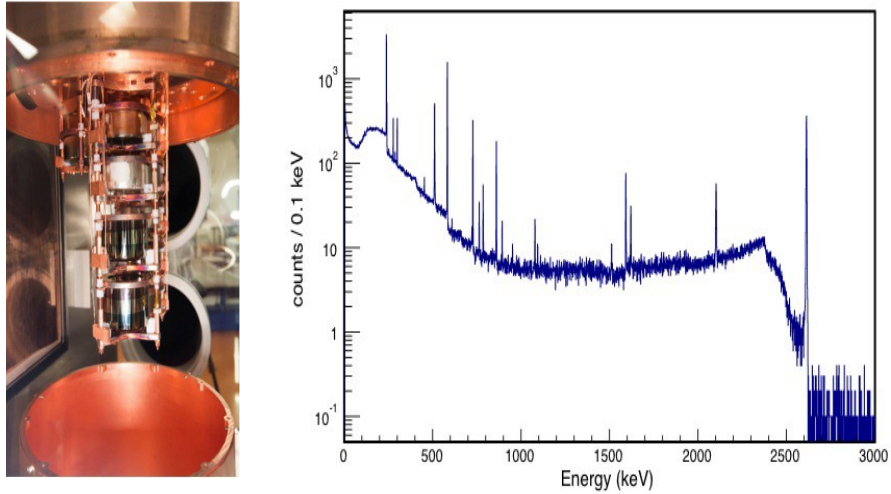


Figure 6: Left: a photograph inside the prototype cryostat which is opened up to allow the mounting of three strings of HPGe detectors. Right: a spectrum taken by one of the HPGe detectors in the prototype cryostat during in a calibration run with a ^{228}Th source.

128 The construction of the DEMONSTRATOR is organized in three phases. In
 129 the first phase, a prototype cryostat made of commercial OFHC copper with
 130 three strings of natural HPGe detectors was constructed in 2013 and has
 131 been in commissioning. The goal of this prototype is to demonstrate the
 132 integration of the various components (detectors, vacuum, cooling, shield-
 133 ing, data acquisition). Most of the natural Ge detectors are the Broad En-
 134 ergy Ge detectors (BEGe) manufactured by Canberra [20], and all of the
 135 enriched Ge detectors and two natural Ge detectors are manufactured by
 136 AMETEK/ORTEC [21].

137 Ten natural HPGe detectors of both BEGe and ORTEC types are ar-
138 ranged into three strings and mounted onto the cold plate inside the pro-
139 totype module cryostat. DAQ systems based on the Object-Oriented Real-
140 time Control and Acquisition (ORCA) platform [22] have been instrumented
141 to control both commercial and collaboration-manufactured electronics, and
142 background data and calibration data are being taken. The HPGe detectors
143 in the prototype cryostat have shown good energy resolution similar to that
144 in commercial cryostats. As an example, a spectrum taken by one of the
145 HPGe detectors during in a calibration run with a ^{228}Th source is shown in
146 Fig. 6. The Full Width at Half Maximum (FWHM) at 2615 keV is 3.2 keV.

147 In the second phase, the first module made from electroformed copper
148 will be populated with a mix of natural and enriched HPGe detectors and
149 run inside the completed shield alongside the prototype cryostat. This second
150 phase is anticipated to begin commissioning in September of 2014. Finally, in
151 the third phase, a second cryostat made of electroformed copper and contain-
152 ing only enriched detectors will replace the prototype cryostat in the shield.
153 At the time of this presentation, 25.2 kg of enriched germanium detectors
154 are underground and MAJORANA is aiming for additional ≈ 4 kg of detectors
155 from the recovery of scrap material. All enriched detectors are extensively
156 tested and characterized in their vendor cryostat both at ORTEC[®] and at
157 SURF. The tests include measurements of the mass, impurity concentration,
158 depletion and operating voltages, leakage current, energy resolution, elec-
159 tronic noise, dead layer, relative efficiency compared to a 3x3-inch NaI(Tl)
160 detector, and pulse-shape discrimination performance.

161 Flood measurements are performed with various sources placed 25 cm
162 above the top surface of the cryostat. Data taken with ^{60}Co are used to
163 determine the detector energy resolution at 1332.5 keV and the detection
164 efficiency relative to a 3x3-inch NaI(Tl) detector. The FWHM of all detectors
165 are better than the experimental specification of 2.3 keV, which is shown as
166 the dotted horizontal line (see Fig. 7).

167 Prior to the final installation of the strings in the module cryostats, they
168 are again tested in the a so-called String Test Cryostat (STC). The goal of
169 these tests is on the one hand to check the integrity of the detector, front-
170 end electronics and HV connection after the re-installation of the detector
171 in the MAJORANA mount, and on the other hand, this configuration allows
172 the measurement of the crystal axis orientation of each detector in the string
173 and the homogeneity of the dead layer along the side of each detector. The
174 crystal axis orientation is of particular interest in view of a possible axion
175 search with MAJORANA.

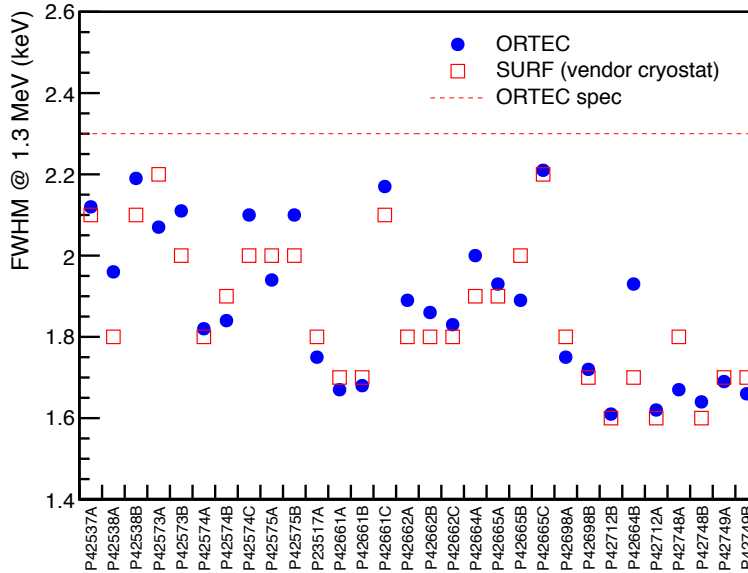


Figure 7: Energy resolution at 1332.5 keV of the 30 enriched detectors measured by ORTEC (dots) and by MJD collaboration at SURF (open squares), plotted against detector serial number.

176 4 Conclusion

177 Developed ultra sensitive ICP-MS assays show that the Cu being electro-
 178 formed underground is clean and the background budget projects to < 3.1
 179 counts/(ROI-t-y). Prototype module with three strings of ^{nat}Ge detectors
 180 was constructed in 2013 and has been in commissioning. All enriched de-
 181 tectors met requirements during characterization in the vendor cryostat at
 182 ORTEC[®] and SURF. At the time of this presentation MAJORANA is in
 183 the process of installing the detectors in specially designed low-background
 184 mounts and strings. First measurements in the string test cryostats show

185 positive results with respects to integrity and performance of the detectors
186 in the MAJORANA mounts.

187 **Acknowledgment**

188 We acknowledge support from the Office of Nuclear Physics in the DOE Office
189 of Science, the Particle Astrophysics Program of the National Science Foun-
190 dation, and the Russian Foundation for Basic Research. We acknowledge
191 the support of the Sanford Underground Research Facility administration
192 and staff.

193 **References**

- 194 [1] *L. Camilleri, E. Lisi, and J. F. Wilkerson* Neutrino Masses and Mixings:
195 Status and Prospects// *Ann. Rev. Nucl. Part. Sci.* 58, 343 (2008)
- 196 [2] *F. T. III. Avignone, S. R. Elliott, and J. Engel* Double beta decay, Ma-
197 jorana neutrinos, and neutrino mass// *Rev. Mod. Phys.* 80, 481 (2008)
- 198 [3] *M. Gell-Mann, P. Ramond, and R. Slansky* Supergravity // North-
199 Holland, Amsterdam, 1979, p. 315
- 200 [4] *R. N. Mohapatra, and G. Senjanovic*// *Phys. Rev. Lett.* 44, 912-915
201 (1980)
- 202 [5] *J. Vergados, H. Ejiri, and F. Simkovic*// *Rept. Prog. Phys.* 75, 106301
203 (2012), 1205.0649
- 204 [6] *L. Baudis et al.* Limits on the Majorana Neutrino Mass in the 0.1 eV
205 Range// *Phys. Rev. Lett.*, 83:41,1999
- 206 [7] *C.E. Aalseth et al.* IGEX ^{76}Ge neutrinoless double-beta decay ex-
207 periment:Prospects for next generation experiments// *Phys. Rev. D*,
208 65:092007, 2002
- 209 [8] *H. V. Klapdor-Kleingrothaus and I. V. Krivosheina* The evidence for the
210 observation of $0\nu\beta\beta$ decay: The identification of $0\nu\beta\beta$ events from the full spectra// *Mod. Phys. Lett. A*, 21:1547, 2006
211

- 212 [9] *M. Agostini et al.* Results on Neutrinoless Double- β Decay of ^{76}Ge from
 213 Phase I of the GERDA Experiment// Phys. Rev. Lett., 111:122503,
 214 2013
- 215 [10] *A. Gando et al.* Limit on Neutrinoless $\beta\beta$ Decay of ^{136}Xe from the First
 216 Phase of KamLAND-Zen and Comparison with the Positive Claim in
 217 ^{76}Ge // Phys. Rev. Lett., 110:062502, 2013
- 218 [11] *J.B. Albert et al.* Improved measurement of the 2 half-life of ^{136}Xe with
 219 the EXO-200 detector// Phys. Rev. C, 89:015502, 2014
- 220 [12] *G.J. Feldman, and R.D. Cousins*// Phys. Rev. D 57, 3873-3889 (1998)
- 221 [13] *F. Simkovic, A. Faessler, H. Muther, V. Rodin, and M. Stauf*// Phys.
 222 Rev. C 79, 055501 (2009)
- 223 [14] *N. Abgrall et al.* The Majorana Demonstrator Neutrinoless Double-Beta
 224 Decay Experiment// Adv. High En. Phys. 2014: 365432, 2014
- 225 [15] *E.W. Hoppe et al.*// J. Radioanal. Nucl. Chem. 282, 315 (2009)
- 226 [16] *P.N. Luke, F.S. Goulding, N.W. Madden, and R.H. Pehl* Low capaci-
 227 tance large volume shaped-field germanium detector// IEEE Transac-
 228 tions on Nuclear Science 36, 926 (1989)
- 229 [17] *P.S. Barbeau, J.I. Collar, and O. Tench* Large-mass ultralow noise ger-
 230 manium detectors: performance and applications in neutrino and as-
 231 troparticle physics// JCAP, 2007, 9 (2007)
- 232 [18] *D. Budjas, M.B. Heider, O. Chkvorets, N. Khanbekov, and S. Schon-*
 233 *ert*// 2009 JINST 4 P10007
- 234 [19] *R. Cooper et al.*// Nucl. Instr. and Meth. A 629, 303 (2011)
- 235 [20] *Canberra Industries, Meriden, Conn, USA, 2009*
- 236 [21] *ORTEC, Oak Ridge, Tenn, USA, 2009*
- 237 [22] *M.A. Howe et al.*// 2004 IEEE Transactions on Nuclear Science 51 878